Applied Catalysis B: Environmental 128 (2012) 91–104

Contents lists available at SciVerse ScienceDirect

Applied Catalysis B: Environmental

journal homepage: www.elsevier.com/locate/apcatb

The role of electron transfer in photocatalysis: Fact and fictions

Hanan H. Mohamed[a,b], Detlef W. Bahnemann[b,*]

[a] Chemistry Department, Faculty of Science, Helwan University, Helwan, Cairo, Egypt
[b] Institut für Technische Chemie, Leibniz Universität Hannover, Callinstrasse 3, D-30167, Hannover, Germany

ARTICLE INFO

Article history:
Available online 5 June 2012

Dedicated to Prof. Dr. Jean-Marie Herrmann on the occasion of his 65th birthday.

Keywords:
Electron transfer
Photocatalysis
Electron dynamic techniques
Kinetic aspects
Mechanistic perspectives

ABSTRACT

Interfacial electron transfer at semiconductor nanoparticles is a fundamental process that is relevant to many applications in photocatalysis such as wastewater cleaning, air cleaning and energy production. Fundamental understanding of the dynamic of the electron transfer is of crucial importance for the understanding of the fundamental concepts of photocatalytic processes and hence results in understanding and industrialization of photocatalytic reactions as well as a rational design of the photocatalytic systems.

This review summarizes the progress in understanding electron transfer dynamics from semiconductor nanoparticles to the electron acceptor molecules. The approaches to improve the electron transfer efficiency will be also reviewed. Of particular focus will be the advancement of methodology as well as overview of some new highlights in electron transfer reactions at TiO_2/liquid interface.

1. Introduction

Photocatalysis using semiconductor nanoparticles have been the subject of research for many decades [1–7]. Recently, nanomaterials have attracted considerable renewed attention because of their promise in many current and potential applications such as electronic devises, sensors and catalysts [8–13]. Depending on where the initial photo-excitation occurs, photocatalysis can be generally divided into two classes of processes. When the initial photo-excitation takes place on the catalyst and the photoexcited catalyst then transfers an electron or energy into a ground state molecule, the process is referred to as a catalyzed photoreaction (Fig. 1(a)). When the initial photoexcitation occurs in an adsorbate molecule (e.g., dye molecules) which then interacts with the ground state catalyst, the process is referred to as a sensitized photoreaction (Fig. 1(b)). The initial excitation of the system is followed by subsequent electron transfer and/or energy transfer.

The principle of the catalyzed photoreactions on semiconductors nanoparticles has been investigated over the past 20 years [1–7,14]. Once electron/hole pairs are generated by light excitation, most of them recombine generating heat. Only a small fraction can successfully transfers to the interface to initiate redox reactions. The time scale of the interfacial electron transfer and the life time of photogenerated charge carrier determine the efficiency of photocatalytic processes. Electron photogeneration and recombination and electron transport are the elementary processes accounting for the conversion of light energy into useful charge carriers. Hence, increasing the efficiency of charge separation/transport in semiconductor nanoparticles is one of the major problems in photocatalysis to be addressed.

Charge carrier transfer has been widely acclaimed to be very important as it plays a pivotal role in photocatalytic processes. The fundamental study of the dynamics of the charge transfer processes is important in the design of new photocatalysts as well as for the industrialization of the photocatalytic processes. Electron transfer process is of great importance for the performance of electronic devices such as solar cells and sensors as well as in the photocatalytic processes such as photosynthesis and water remediation of organic (e.g., dye compounds, phenolic compounds) and inorganic contaminants (e.g., toxic metal ions).

A use of time resolved spectroscopy covering the time scale from picoseconds to millisecond and spectral range in the UV and visible light is a powerful tool to study the light induced electron transfer processes and provide mechanistic information voluble for design of novel and optimized materials. During the past decades, extensive investigations have been performed concerning the study of the kinetics and of the mechanistic details of the interfacial electron transfer processes at the semiconductor/water interface using the laser photolysis [14–16] and the pulse radiolysis technique [17–20]. Recently, stopped flow technique has been employed to study the dynamics of one and multi-electron transfer reactions at TiO_2 nanoparticles [21–24].

In this article an overview on the charge carrier dynamics at semiconductor nanoparticles will be provided. The experimental techniques for nanoparticles synthesis, characterization as well as the development in the measurements of interfacial electron

* Corresponding author. Tel.: +49 5117625560; fax: +49 5117622774.
E-mail address: bahnemann@iftc.uni-hannover.de (D.W. Bahnemann).

0926-3373/$ – see front matter © 2012 Elsevier B.V. All rights reserved.
http://dx.doi.org/10.1016/j.apcatb.2012.05.045

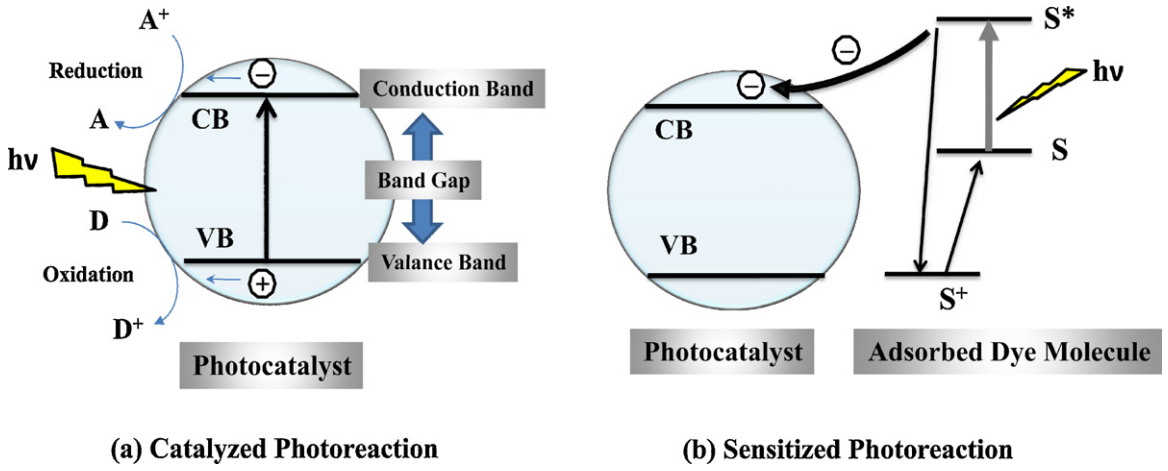

Fig. 1. Schematic presentation of photocatalytic processes.

Adapted from Ref. [74].

transfer dynamics properties will be reviewed. The factors affecting the efficiency of the electron transfer property including the nanoparticle surface, size and morphology will be discussed in detail. Of particular interest will be the new findings in dynamic study of some important electron transfer reactions at TiO_2 nanoparticles. Comparison and contrast will be made between different employed methods. A future direction and a summary will be given at the end of the article.

2. Kinetic aspects

2.1. Dynamics of charge carrier trapping and recombination

Exciting a semiconductor with any light source causes interband transition, excitonic transition or below-band gap transitions. If the photon energy is larger than the band gap, interband transitions dominate, exciting electrons from the valence band into the conduction band in the fs timescale (Eq. (1)). Tamaki et al. [25] have proposed that the electrons and holes walk randomly to the surface of the photocatalyst and are trapped there in the sub-ps timescale (Eq. (2a)). Electron and hole can also be trapped at bulk trapping sites (Eqs. (2b) and (2c)). Tamaki et al. [25] suggested that electrons are capable of migrating between the surface and the bulk traps that are in equilibrium since these species are energetically equivalent and probably very close to the conduction band edge. Fig. 2 shows the energy levels for the surface trapped electrons and bulk electrons suggested from the surface relaxation dynamics. At the surface of the photocatalyst the trapped electron and hole can recombine at surface (Eq. (3)) or rather transfer to acceptor (A) or donor (D) molecules, respectively and react with them (Eq. (4)). After the charge transfer back reaction between the reduced acceptor and hole or oxidized donor and electron can occur when the species are strongly adsorbed to the surface [26–28]. The recombination of electrons and holes is an important electronic process in semiconductors. Rectification, photoconductivity, and transistor behavior are critically dependent on the life time of the injected mobile carriers. The recombination rate also plays a critical role in photocatalytic reactions with semiconductor particles.

Hoffmann et al. [3] summarized a general mechanism of heterogeneous photocatalysis on TiO_2 by the following steps (cf. Fig. 3):

(1) Charge carrier generation

$$TiO_2 + h\upsilon \rightarrow h_{VB}^{+} + e_{CB}^{-} \quad (fs) \tag{1}$$

(2) Charge carrier trapping

$$e_{cb}^{-} + > Ti^{IV}OH \rightarrow \{> Ti^{III}OH\} \quad \text{shallow trap} \quad (< 200\,ps) \tag{2a}$$

$$e_{CB}^{-} + > Ti^{IV} \rightarrow > Ti^{III} \quad \text{deep trap} \quad (10\,ns) \tag{2b}$$

$$h_{VB}^{+} + > Ti^{IV}OH \rightarrow \{Ti^{IV}OH^{\bullet}\}^{+} \quad (10\,ns) \tag{2c}$$

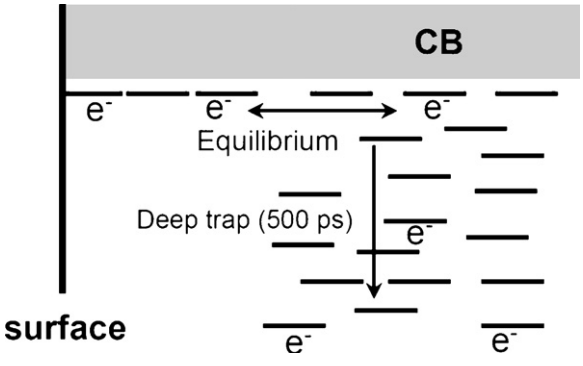

Fig. 2. Schematic illustration of spatial and energetic distribution of electron traps in the TiO_2 films.

Reprinted with permission from Ref. [25(a)].
© 2007 RSC

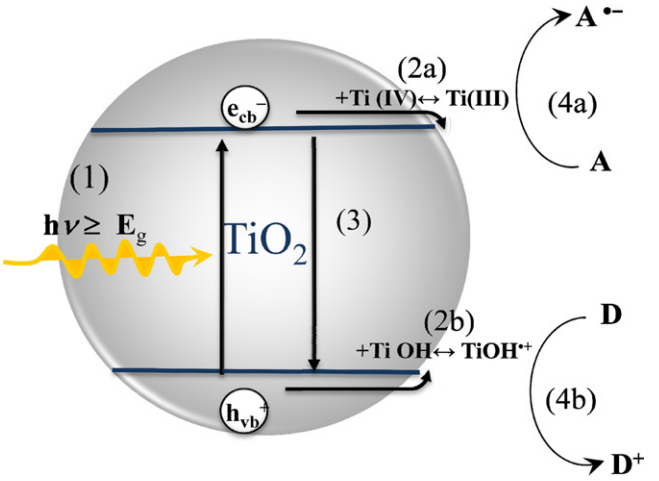

Fig. 3. Schematic representation of the general mechanistic steps in heterogeneous photocatalysis on TiO_2 nanoparticles.

Adapted from Ref. [74].

Table 1
Summary of some measured characteristic time for primary processes in photocatalysis at various TiO_2 particles.

Primary process	Characteristic time	Sample description
Charge carrier generation		
$TiO_2 + h\nu \rightarrow e^- + h^+$	fs	
Charge trapping		
$h^+ \rightarrow h_{tr}^+$	<200 fs	Nanoporous film [25(a)]
$e^- \rightarrow e_{tr}^-$	<150 fs	
$h_{s\text{-}tr}^+ \rightarrow h_{d\text{-}tr}^+$ (relaxation)	~100 ps	
$e_{s\text{-}tr}^- \rightarrow e_{d\text{-}tr}^-$ (relaxation)	~500 ps	
Charge recombination		
$e^- + h_{tr}^+$, $h^+ + e_{tr}^-$ or $h^+ + e^- \rightarrow$	1 μs	Nanoporous TiO_2 film (water) [29(b)]
Heat (or $h\nu$)	25 μs	Nanoporous TiO_2 film (air) [26]
Interfacial charge transfer		
	~300 ps (methanol oxidation)	Nanoporous TiO_2 film [25(b)]
	~3 ns (2-propanol oxidation)	Nanoporous TiO_2 film [25(b)]
	<2 μs (water oxidation)	Degussa P25 powder [29(c)]
h^+(or h_{tr}^+) + Red → Red^+	No water oxidation within 80 μs	Nanoporous TiO_2 film [29(d)]
$e_{tr}^- + O_2 \rightarrow O_2^-$	<100 ns	Nanoporous TiO_2 film [29(b)]
$e^- + O_2 \rightarrow O_2^-$	10–100 μs	Degussa P25 powder [29(c)]
$e^-(ore_{tr}^-) + O_2 \rightarrow O_2^-$	~10 μs	Nanoporous TiO_2 film [26]
$e^- + Pt \rightarrow e^- \ldots Pt$	2.3 ps	Degussa P25 powder [29(e)]

Reproduced with permission from ref. [29(a)]. © 2008 Elsevier.

(3) Charge carrier recombination

$$e_{CB}^- + \{> Ti^{IV}OH^\bullet\}^+ \rightarrow Ti^{IV}OH \quad (100\,ns) \tag{3a}$$

$$h_{VB}^+ + \{> Ti^{III}OH\} \rightarrow Ti^{IV}OH \quad (10\,ns) \tag{3b}$$

(4) Interfacial charge transfer

$$\{> Ti^{III}OH\} + A \rightarrow \{> Ti^{IV}OH\} + A^{\bullet -} \quad (ms) \tag{4a}$$

$$\{> Ti^{IV}OH^\bullet\}^+ + D \rightarrow \{> Ti^{IV}OH\} + D^{\bullet +} \quad (100\,ns) \tag{4b}$$

Fujishima et al. [29(a)] summarized the processes occurring on TiO_2 particles after UV irradiation and the characteristic surface reactions and their time scale in Table 1 [25,26,29(a–e)] and Fig. 4 [29(a)].

According to the above mechanism the interfacial charge transfer efficiency is limited by two important processes: the competition between charge carrier recombination and trapping followed by the competition between trapped carrier recombination and interfacial charge transfer.

2.2. Trapped versus free charge carriers in semiconductor particles

The distribution of charge carriers between the conduction band and trapping states is an important phenomenon. Heterogeneous photochemical charge transfer reactions are often performed with semiconductor nanoparticles containing trapping sites in the bulk and at the surface. After charge separation in the absence of suitable adsorbed hole scavengers and the presence of molecular oxygen (i.e., an electron scavenger) the remaining holes oxidize surface water to produce adsorbed hydroxyl radicals which can subsequently induce further oxidation reactions. However, in the presence of an adsorbed hole scavenger such as methanol and in the absence of molecular oxygen the fate of the photogenerated electrons is still not clear. Bahnemann et al. [14] reported that excess electrons are trapped close to the surface of colloidal particles forming Ti^{3+} which is characterized by broad absorption spectra with λ_{max} = 650 nm while trapped holes oxidize the surface water producing the surface adsorbed hydroxyl radical with the absorption at 460–500 nm. O'Regan et al. [30] observed near infrared absorbance spectra when TiO_2 membranes were biased at a negative potential. The authors attributed these absorbance spectra to free conduction band electrons with only a small fraction of the electrons being trapped at surface sites. Boschloo and Fitzmaurice [31] reported that the optical absorption of trapped electrons produced in TiO_2 nanocrystalline layers under negative applied potential is strongest at 400 nm and gradually decreases to 0 at 600 nm which is superimposed with the visible absorption spectrum of conduction band electrons that is observed when applying a more negative potential. The authors determined the extinction coefficient of an electron trapped in a surface state to be 1900 $M^{-1}\,cm^{-1}$ at λ_{max} = 400 nm, more than three times higher than that of conduction band electron at the same wavelength. This evince that the absorption of trapped electrons is most pronounced near 400 nm [32]. Those authors proposed an average of 12 traps per TiO_2 nanocrystal of 12 nm diameter. Safrany et al. [32] observed a shift in the absorption spectra of TiO_2 electrons to longer wavelength after longer time illumination. They attributed this to the storing of electrons in the conduction band after the traps have been filled.

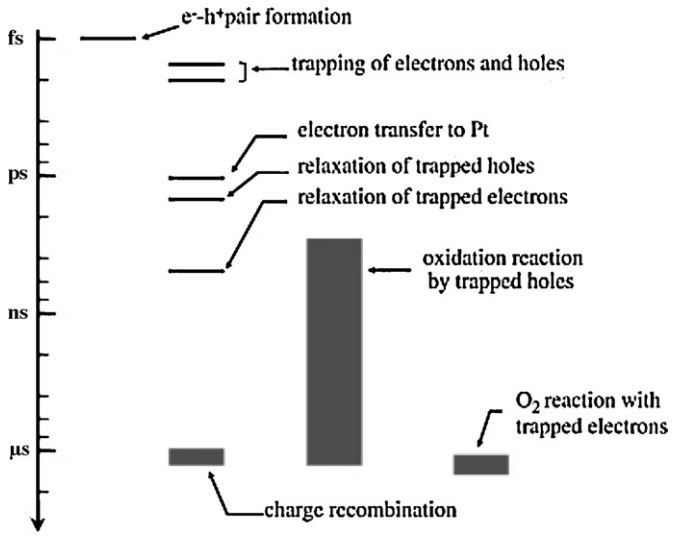

Fig. 4. Time scales in photocatalysis on bare TiO_2 particles. Reprinted with permission from Ref. [29(a)]. © 2008 Elsevier.

3. Experimental techniques

3.1. Synthesis and characterization of semiconductor nanoparticles

There are several methods to prepare semiconductor particles ranging from simple chemical method such as sol–gel method to mechanical and vacuum method. The experimental details of the preparation methods are not of our interest in this article. However, it is important to specify some limitations of using semiconductor nanoparticles in aqueous solution for the performing the spectroscopic dynamic studies. For absorption measurements it is important to use transparent colloidal suspension, so that light scattering of the particles is negligible. This can be achieved using

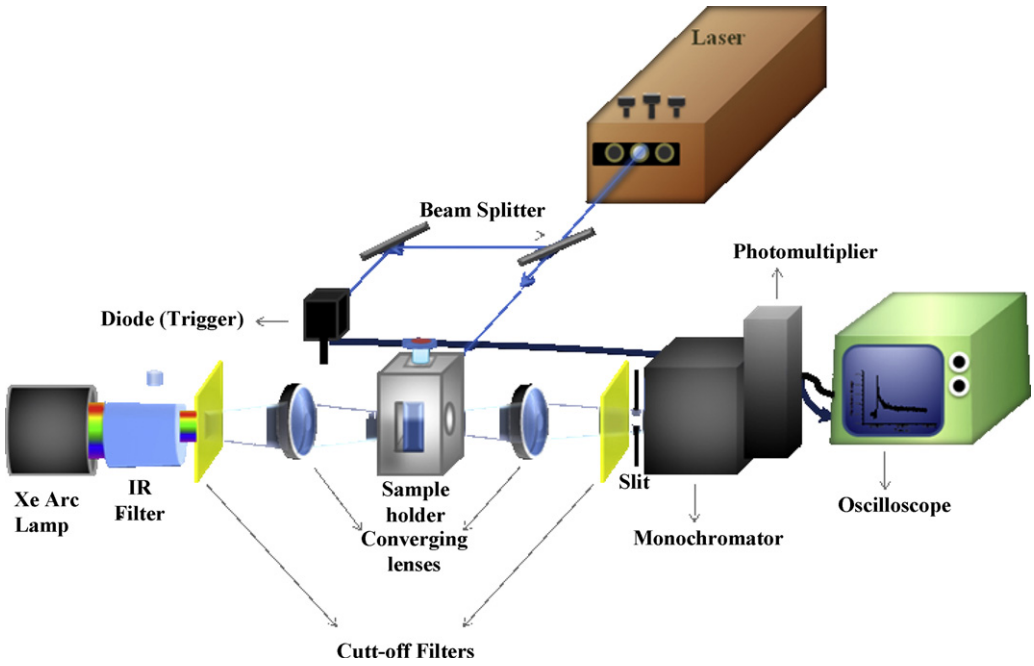

Fig. 5. Schematic representation of the set-up of a Nanosecond laser flash photolysis spectrometer. Adapted from Ref. [74].

suspensions of extremely small sizes of semiconductor particles. Kormann et al. [33] have employed a simple hydrolysis method to prepare transparent colloidal suspensions of TiO_2 nanoparticles (2–3 nm particle size) from the inorganic precursor. Transparent colloidal TiO_2 suspensions were also prepared from organic precursor (Titan(IV)-isopropoxid) according to Bahnemann el al. [34] Moreover, since TiO_2 systems used frequently in photocatalytic applications are not transparent solutions but powder or opaque suspensions time-resolved diffuse reflectance spectroscopy can be employed [35–39]. The second limitation is that the TiO_2 particles is soluble in water over only small pH range and therefore, it is necessary to use a stabilizing agent such as polyvinyl alcohol (PVA) [40] for the particles employed under pH higher than 3.

Properties of nanoparticles have been characterized using a variety of techniques including spectroscopy, microscopy, and X-ray techniques. Most studies have focused on their equilibrium properties, such as optical absorption and emission, particle shape, surface structure and interparticle interaction [41–47]. Surface properties of nanoparticles have been studied using various types of spectroscopy, such as electronic absorption [48,49], Fluorescence [50–53], IR [54], and Raman [47,55]. The particle size and shape can be characterized by transmission electron microscopy (TEM), scanning tunneling microscopy (STM), and atomic force microscopy (AFM) [41,53,56,57]. With high resolution microscopy such as HRTEM, crystal lattice structures, and grain boundaries of nanoparticles can be clearly determined.

3.2. Measurements of interfacial electron transfer dynamics

3.2.1. Laser flash photolysis technique

Time resolved laser flash photolysis technique is one of the most frequently employed techniques for the measurement of the charge carrier transfer dynamics at semiconductor nanoparticles [14–16]. The basic approach is to excite the semiconductor nanoparticles with short femtoseconds to nanosecond laser pulses generated from ultrafast laser system. The excited charge carriers are then monitored with continuous light beam. The change in the absorption of the continuous light reflects the change in the population of the excited state charge carriers. A schematic diagram of a typical time resolved laser setup used for the dynamics of charge carrier transfer at semiconductor nanoparticles is shown in Fig. 5.

3.2.2. Pulse radiolysis technique

This technique is a common method of initiating fast reactions to study reactions occurring on a timescale faster than approximately 100 ms. The technique involves exposing a sample of material to a beam of highly accelerated electrons. In aqueous solution the radiolysis results in the formation of e_{aq}^-, $H^\bullet$, $OH^\bullet$...etc. Pulse radiolysis has been recently used to study the dynamics of electron transfer reactions from TiO_2 nanoparticles to various electron acceptors [17–20]. Reactions of the hydrated electron, H atoms, 2-propanol, and methanol radicals with the TiO_2 nano-particles have been studied either directly or by competition kinetics [17]. The radicals were produced by radiolysis of 2-propanol, *t*-butanol, or methanol aqueous solutions in acid pH. The reactions involve the injection of e_{aq}^- to the conduction band of the TiO_2 particle.

3.2.3. Electron paramagnetic resonance (EPR) technique

EPR is an useful technique to probe the dynamics of the charge separation and therefore photocatalytic behavior in TiO_2 either directly [58] or by spin trapping methods [59]. Using this technique one can not only monitor trapped electrons in localized states but also holes trapped as oxygen anion O^- centers which are EPR active (Fig. 6) [60]. Hurum et al. have studied the UV light induced charge separation characteristics in mixed phase titania photocatalyst (Degussa P25) by EPR spectroscopy [61]. In a common low temperature EPR experiments (i.e., illumination of semiconductor such as TiO_2 at 4 K), the energy is not enough for the diffusion of the photogenerated charges from trapping sites. The hole rapidly migrates to the surface trapping sites wile electrons are initially observed primarily in Ti(III) lattice trapping sites. Since the structural geometry of the rutile and anatase are sufficiently different, the paramagnetic properties of trapped electrons in the two phases are distinct and can be resolved EPR. With this technique subsequent migration of electron/hole pairs was examined by measuring the changes in local symmetry and spin lattice

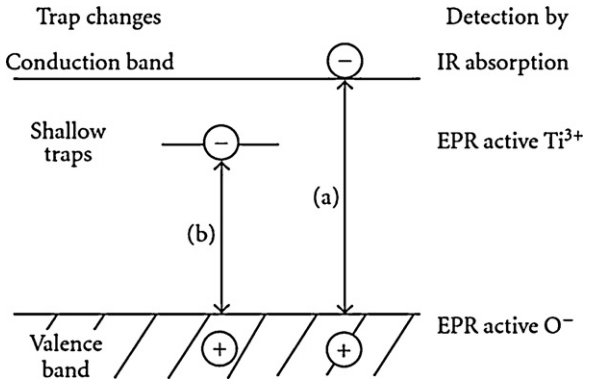

Fig. 6. Scheme of UV induced charge separation in TiO_2. Electrons paramagnetic resonance spectroscopy detects both electrons in shallow traps Ti(III) and hole centers O^-.

Reprinted with permission from Ref. [60].
© 2005 ACS

interactions which provide detailed molecular information about charge transfer behavior among the TiO_2 phases.

A combination of EPR and IR Spectroscopy measurements was used to study electron/hole excitations in anatase TiO_2 powders [60]. During continuous UV irradiation in the mW cm^{-2} range photogenerated electrons are either trapped at localized sites, giving paramagnetic Ti(III) centers, or remain in the conduction band as EPR silent species which may be observed by their IR absorption.

3.2.4. Photoluminescence measurements

Photoluminescence (PL) spectroscopy is a highly sensitive tool to study the electronic properties of the photogenerated electron/hole pairs in TiO_2 nanoparticles [62–65]. Photoluminescence of semiconductor nanoparticles originates from recombination of electron/hole pair. Photoluminescence of the vacuum-deposited films was observed upon excitation by UV irradiation at 77 K, while the emission is hardly detectable at room temperature. It was shown that the SiO_2/TiO_2 multilayer film with 20 nm set-thick over layer exhibits more intense luminescence than those from the bare TiO_2 film and the multilayer film with 10 nm set-thick over layer and all the films have broad emission bands peaked around 550 nm [64]. The spectra upon excitation at 350 and 266 nm show similar spectral features but their emission intensities are significantly different from each other. The broad luminescence observed in the visible region is probably due to emission from self-trapped excitons (electron–hole pairs) localized on the TiO_6 octahedron [66] and/or transition from charge-transfer excited states (Ti^{3+}—O^-) in trap sites [67]. Recently, the photon energy up-conversion (UC), (i.e., the emission at energies higher than the excitation energy) has been intensively studied in bulk semiconductors [68,69] as well as semiconductor quantum dots [70]. In bulk semiconductors the proposed mechanism involves either a two-step photoexcitation process [71] or an Auger recombination [72]. In semiconductor quantum dots is based on surface and phonon processes [73].

3.2.5. Stopped flow technique

It is one of the techniques used to study the kinetics of reactions which are take place in the solution in the millisecond time scale. Stopped flow technique has been recently used to study the one and multi-electron transfer reactions occurring at the surface of TiO_2 nanoparticles [21–24,74]. In a typical stopped flow experiment (cf. Fig. 7), nanosized TiO_2 particles loaded with electrons were injected in one of the stopped flow syringes and the electron acceptor (e.g., $O_2(H_2O)$, H_2O_2, $N_2(H_2O)$, ...) was injected in the other syringe. A 1:1 mixing of the two reactants takes place and the resulting reactant mixture travels to the optical cell where the change in the absorbance with time is measured. The kinetics of the electron transfer reactions was studied by following the decay of the absorbance of TiO_2 electrons at 600 nm or the build-up of the absorption signals of products.

4. Factors affecting electron transfer efficiency

The key to improve photocatalytic activity depends on the photocatalyst size [75], surface composition [76], and morphology [77]. There have not been yet systematic studies on the effects of the particle size and morphology on the electron transfer efficiency. This is largely because of the difficulty of preparing single-size, single-shape particles with uniform and well defined surface properties. However, the results reported to date suggest that the efficiency of electron transfer reactions depends largely on these properties.

4.1. Effect of nanoparticle surface and size

Enhancement of the electron transfer efficiency at semiconductor particles can be improved by surface modifications. The surface of the semiconductor particle can be modified by various methods

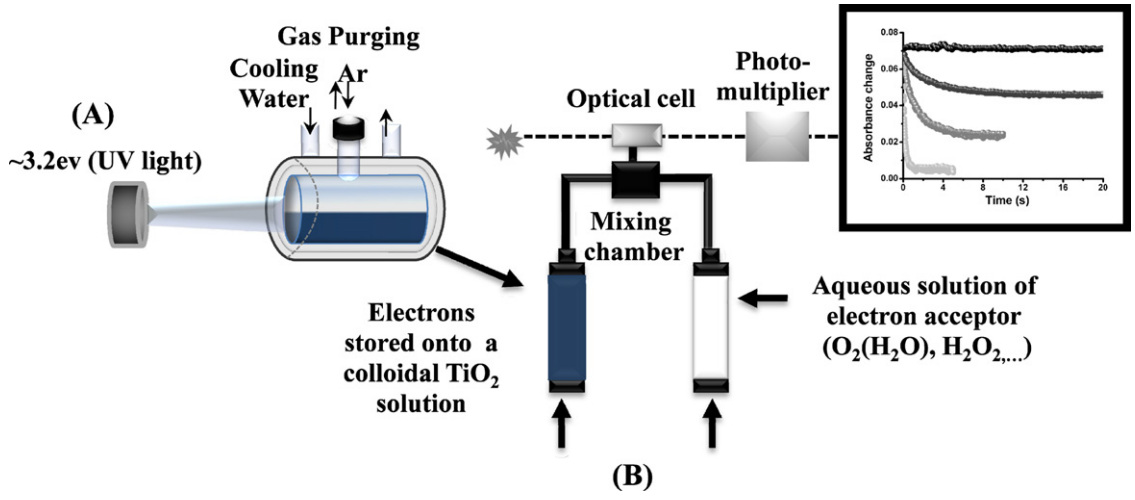

Fig. 7. Schematic illustration of the stopped flow experiment for the multi-electron transfer reactions induced by stored electrons in TiO_2 nanoparticles.
Reprinted with permission from Ref. [22].
© 2011 ACS

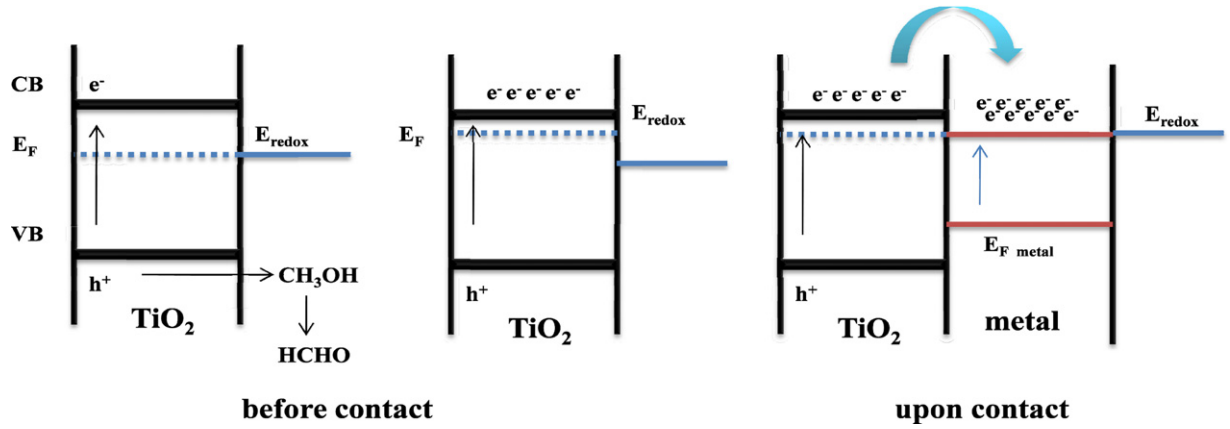

Fig. 8. Equilibration of semiconductor–metal nanocomposites with a redox couple before and after irradiation. Electron storage in metal nanoparticles causes the Fermi level to shift closer to conduction band of the semiconductor.
Adapted from Ref. [74].

such as deposition of noble metal clusters [78], doping of transition metal ions [79], surface complexation [80] and semiconductor coupling [81]. Particularly, the small dimension of the particle (less than 10 nm) results in perturbation of the band structure of the semiconductor particle; the small semiconductor particles show different photophysical properties from those of bulk materials which is commonly known as "quantum size effect" [8]. In very small colloidal particles, the energy levels are quantized, the spacing between adjacent states being of the order of E_F/N, where E_F is the Fermi energy and N is the number of atoms in one particle. Since E_F has a value of a few eV, the energy levels in a particle containing about 10^4 atoms are about 10^{-4} eV.

Under band gap excitation of the semiconductor particle, the charge carriers are separated. Due to the small size of the particles and the high recombination rate only a small fraction of these charge carriers (~5%) can be used to undergo redox reactions at the interface. One of the promising strategies to overcome the limitations in achieving higher photoconversion is the adequate deposition of a transition metal on semiconductor nanoparticles. Upon contact, a Schottky barrier can be formed between the semiconductor and the metal particle, leading to a rectified charge carrier transfer. Efforts to employ semiconductor–metal composite nanoparticles have been explored to facilitate charge rectification in the semiconductor nanostructures and improve the interfacial charge transfer efficiency [82–89,81].

Upon band gap irradiation of the semiconductor nanoparticles electrons generated in the conduction band raises its Fermi level to more negative values [90]. Then, the energetic difference at the semiconductor/metal interface drives the electrons from the conduction band of the semiconductor into the metal nanoparticles. Upon sufficient charge accumulation, the Fermi levels of the two components can equilibrate at a potential that is progressively shifted to more negative values with increasing electron density (Fig. 8) [91,92]. In general, only composite systems establishing ohmic metal– solution contact act as efficient catalysts for quick e_{CB}^- migration to the solution (Pt or Pd). Conversely, in the presence of non-ohmic interfaces (e.g., with Ag, Au, Cu), excess e_{CB}^- can remain stored effectively on both components of the nano-junction under suitable conditions [93,94]. This altered energetic path plays a fundamental role in modulating the overall photocatalytic activity of semiconductor–metal composite systems [95,96].

Doping of transition metal species is another approach to inhibit electron–hole recombination during illumination and consequently increasing the lifetime of the photogenerated electrons. Using this approach one can also harvest the photons in the visible light. It was found that doping of TiO_2 with Fe^{3+} resulted in the increase in Ti^{3+} intensity which was observed by ESR upon photoirradiation [97]. It is believed that the doping transition metals create mid-gap states where direct recombination occurs. A promising process is the doping of semiconductor particles with nonmetals such as nitrogen [98], carbon [99], fluorine [100] and iodine [101].

Charge carrier seperation of semiconductor nanoparticle can also be improved by coupling with another semiconductor particle. CdS–TiO_2 composite nanoparticles is one of the early studied system [102(a,b)]. According to the energytic model illustrated in Fig. 9 [102(a)], a short band gap semiconductors (1) absorbs the photons in the visible light. The resulted photogenerated electron will be subsequently transferred to the large band gap semiconductors (2). This study highlights the benefits of charge carrier rectification between the two semiconductor nanoparticles which improve the overall efficiency of the photocataltic system. Similar nanocomposite systems such as ZnO–CdS [102(c)], TiO_2–SnO_2 [103], SnO_2–CdSe [104], and SnO_2–CdS [105] have been efficiently used to promote efficient charge separation and charge propagation in dye-sensitized solar cells.

Makarova et al. [106] found that surface modification of nanocrystalline TiO_2 with electron-donating chelating agents (i.e., arginine-modified TiO_2) is an effective route to enhance photodecomposition of nitroaromatic compounds. Obare et al. [107] have described a new applicable approach for enhancing the photocatalytic multi-electron transfer by anchoring well-defined molecular catalysts (hemes) to mesoporous nanocrystalline TiO_2

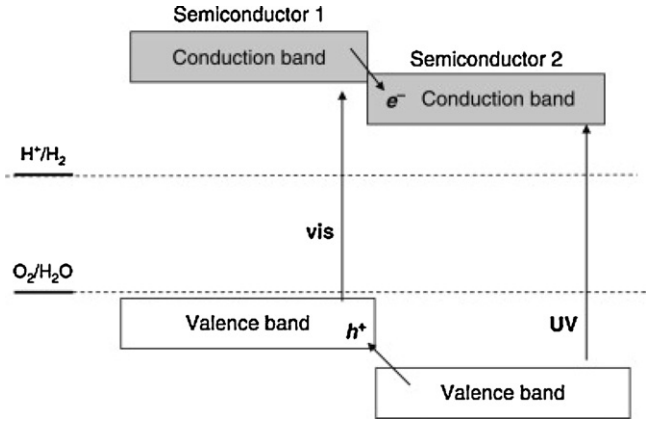

Fig. 9. Photoexcitation in composite semiconductor-semiconductor photocatalyst. Reprinted with permission from Ref. [102(a)].

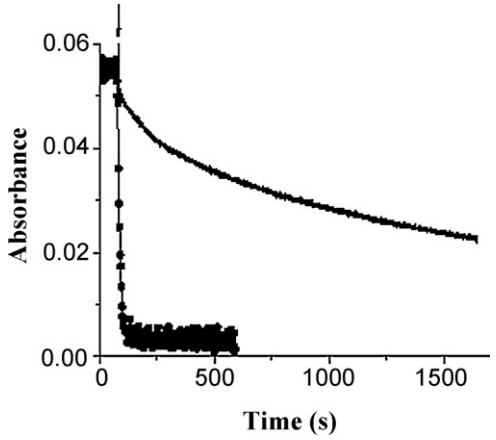

Fig. 10. Absorbance at 1000 nm of heme/$TiO_2(e^-)$ (•••) and $TiO_2(e^-)$ (–) as a function of time. The arrow indicates the point at which 1,2-dichlorobenzene was added to the external methanol solution.
Reprinted with permission from Ref. [107].

thin films. Heme-functionalized nanocrystalline TiO_2 was found to trap, store, and transfer multiple electrons to organohalide pollutants. The authors found that the rate of the reactions mediated by heme/$TiO_2(e^-)$ was 80–150 times larger than $TiO_2(e^-)$ in the absence of heme (Fig. 10). In this system a synergy between the molecular catalysts and the semiconductor was observed. The mechanism of organohalide reduction mediated by Heme functionalized TiO_2 system is illustrated in Fig. 11 and described by the following equations [108,109].

$$\text{Heme/TiO}_2(ne^-) + \text{RX} \rightarrow \text{Hemin/TiO}_2(ne^-) + \text{RX}^{\bullet -} \quad \text{slow} \quad (5a)$$

$$\text{Hemin/TiO}_2(ne^-) \rightarrow \text{Heme/TiO}_2((n-1)e^-) \quad \text{fast} \quad (5b)$$

$$\text{Heme/TiO}_2 + \text{RX} \rightarrow \text{Hemin/TiO}_2 + \text{RX}^{\bullet -} \quad (5c)$$

4.2. Effect of morphology

One of the most important factors affecting the photocatalytic activity of TiO_2 is its specific surface area which is believed to be higher in a continuous structure rather than in discrete particle. This can be attributed to the easier electron transfer within the continuous structure [110]. In the light of that, mesoporous semiconductor materials have attracted much interest for improving the electron transfer efficiency and the overall photocatalytic activity. Mesoporous nanostructures materials offer a powerful approach for tailoring the electron transport property and charge separation ability. This can be attributed to the larger specific surface area of mesoporous TiO_2 versus discrete nanoparticles, so that rapid diffusion of the charge carriers takes place through 3-D mesoporous TiO_2 network by the so called antenna mechanism. The photogenerated electrons transferring from the location of light absorption to a suitable interface where the actual electron transfer reaction will take place (Fig. 12) [110]. Moreover, the smaller crystal sizes of the TiO_2 particles consist the mesoporous structure are also useful for the photogenerated electron/hole pair separation.

Mesoporous nanostructure synthesis has been a search of interest since 1995 [110]. Many efforts have been made to modify the mesoporous nanostructure by the deposition of noble metal clusters such as Pt, Au, Ag [111–117], doping with transition metal ions [118,99] or nonmetal such as nitrogen and carbon [119]. Another approach to modify the mesoporous TiO_2 dealing with a new morphology such as nanostructure TiO_2 hollow fibers layers applied in dye-sensitized solar cells (Fig. 13(a)) [120]. This material exhibited remarkably enhanced electron transport properties compared to mesoscopic films made of spherical nanoparticles (Fig. 13(b)) [120].

5. Electron transfer reactions at semiconductor nanoparticles

5.1. Reduction of viologen compounds

Viologen compounds were chosen as model electron acceptors to study the interfacial electron transfer at semiconductor nanoparticles [40,16,121,122]. Viologen compounds (N,N′-dialkyl-4,4′-dipyridinium dichloride) are well known to be subjected to one-electron reduction which produces the blue radical cation ($V^{\bullet +}$) from the colorless dication (V^{2+}) (Eq. (6)). Viologen radical cations have attracted much attention because of their strong redox ability. They are capable of reducing protons to produce molecular hydrogen. In view of this, there has been a surge of interest directed to photocatalytic generation of $V^{\bullet +}$ as a possible means of light-to-chemical energy conversion [123–129]. Viologen compounds are known also for their diverse applications, as a herbicidal and

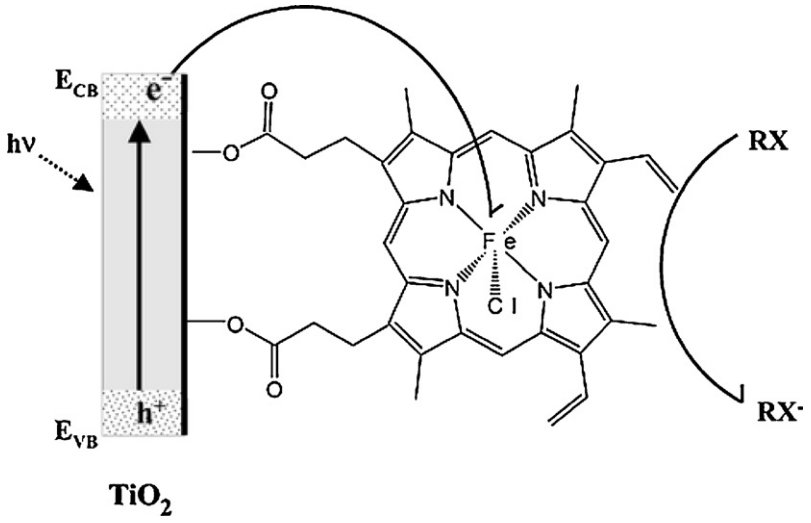

Fig. 11. The possible multi-electron transfer processes of heme/$TiO_2(e^-)$ reaction with organohalide pollutants.
Reprinted with permission from Ref. [108].

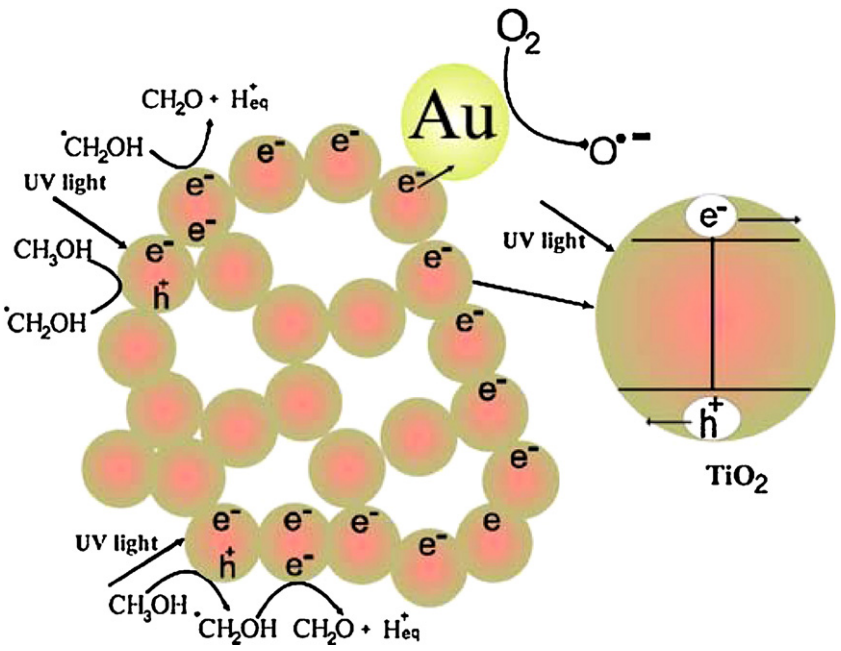

Fig. 12. Schematic illustration of the proposed antenna mechanism to explain the enhanced activity for methanol photooxidation over mesoporous Au/TiO_2 nanocrystals as photocatalysts.

Reprinted with permission from Ref. [110(a)].
© 2009 ACS

toxicological agent [106]. The herbicidal activity of viologen compounds is related to the facile reaction of their radical cations with oxygen generating superoxide radical anions [128–131].

$$V^{2+} + e^- \rightarrow V^{\bullet+} \quad (6)$$

Recently, Mohamed et al. [24,74] studied single- and multi-step electron transfer processes in the presence of viologen compound (methylviologen (MV^{2+}) and benzylviologen (BV^{2+})) as electron acceptors with and without noble metal particles as a second electron acceptor.

Mohamed et al. [24,74] found that the second order rate constant obtained employing stopped flow technique at pH 2.7 ($k = 2.06 \times 10^4\ M^{-1}\ s^{-1}$) was smaller than the value obtained by Duonghong et al. [15] employing laser flash photolysis technique (estimated from the data in Fig. 6 [15] to be about $1 \times 10^5\ M^{-1}\ s^{-1}$ at pH 2.7 (using the data of the first order rate constant of $10^2\ s^{-1}$ and [MV^{2+}] of 10^{-3} M)). While, at the first sight, similar values of the rate constants would be expected as a one electron transfer reaction occurred in both sets of data, in the laser flash photolysis experiments the colloidal suspensions TiO_2 are in equilibrium with adsorbed and bulk MV^{2+} while there is initially no adsorbed MV^{2+} on the TiO_2 surfaces employing the stopped flow technique. Moreover, also the properties of the employed TiO_2 particles are quite different in both studies with different particle sizes and crystallinity.

Mohamed et al. [24,74] observed a subsequent decay of the reduced viologen radicals when metal clusters present (Fig. 14(a)). This seems to indicate a predominant electron transfer process from viologen radical in the solution to the adsorbed hydrogen ions on the surfaces of the metal clusters. The decay of viologen radical

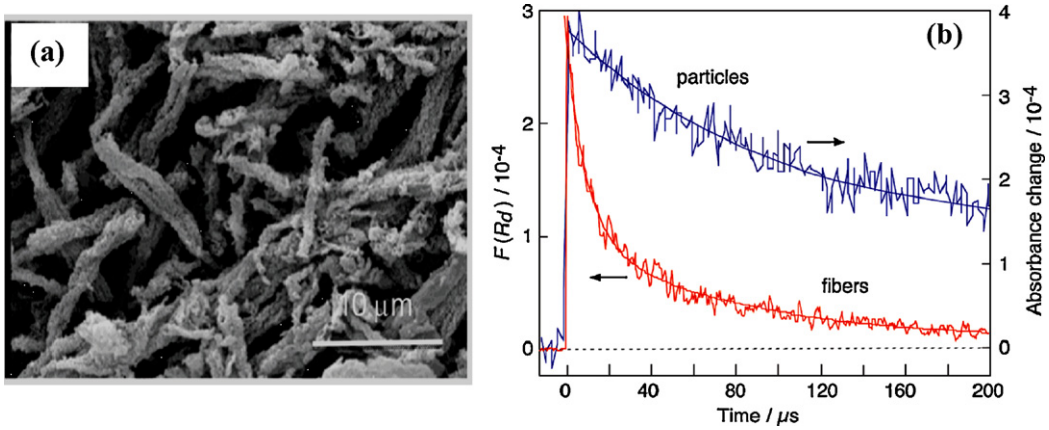

Fig. 13. (a) Typical SEM image of TiO_2 nanofibers obtained after milling and ultrasonication to make a paste. (b) Temporal behavior of the Kubelka–Munk function $F(\Delta R_d)$ of the transient diffuse reflectance measured at $\lambda = 630$ nm for a C101 dye-sensitized, 6 μm thick, TiO_2 fibrous opaque film covered by a redox-inactive ionic liquid upon nanosecond pulsed laser excitation.

Reprinted with permission from Ref. [120].
© 2010 ACS

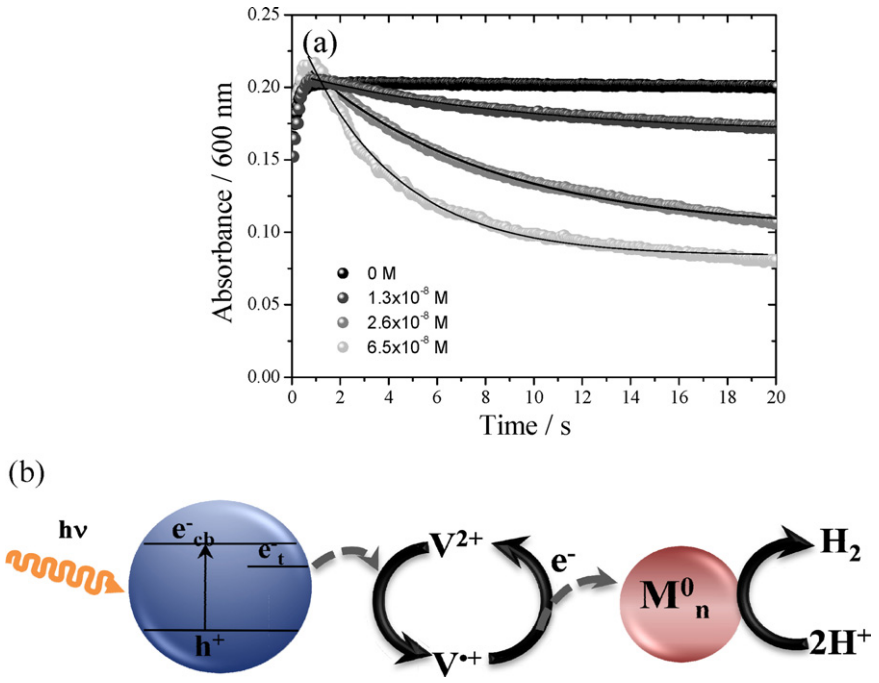

Fig. 14. (a) Time profiles of the formation and decay of the methyl viologen radical absorbance at 600 nm observed upon mixing of electron loaded TiO_2 suspension ($[e_{TiO_2}^-] = 1 \times 10^{-4}$ M) with Ar-saturated methyl viologen dication aqueous solutions (1×10^{-3} M) at pH 2.7 ($[H^+] = 3.2 \times 10^{-3}$ M) in the absence and in the presence of various concentrations of gold metal particles, solid lines represent the first order fits. Schematic illustration of the electron transfer processes from TiO_2 nanoparticles to the viologen dication forming the viologen radical cation and the ensuing electron transfer from the radical cation to the metal particles forming H_2 gas. Adapted from Refs. [24,74].

in the presence of metal particles was suggested to reveal the role of V^{2+} as an electron relay for hydrogen production by transferring the electron between TiO_2 nanoparticles and noble metal particles (Fig. 14(b)).

5.2. Photocatalytic reduction of transition metal ions

The photocatalytic reduction of transition metal ions is an important process because of two effects: (1) the transformation of the ions to less toxic species and (2) the deposition of the reduced metals on the semiconductor catalyst surface for recovery of expensive and useful metals. Moreover, noble metal islands deposited on semiconductor surfaces have unusual catalytic and optoelectronic properties [132]. It is well known that at the nanometer scale, the optical, electronic and catalytic properties of transition-metal nanoclusters are highly sensitive to their size and shape. Whereas deposition of metal nanoparticles improves both charge separation as well as interfacial charge transfer kinetics the mechanism responsible for such an improvement is yet to be understood fully on the nanoscale. One main reason for this paucity of mechanistic information is the lack of the experimental methods able to follow these processes in real time [133]. A fundamental understanding of the kinetics and mechanisms involved in the reduction of metal nanoclusters on nanometer-scale semiconductors is from the fundamental and practical point of view. It is believed that the key of the catalytic properties including selectivity, activity, lifetime and stability [134,135] depend on the catalyst size [136], surface composition and structure [137], which in turn require greater control over catalyst syntheses. The reduction of the metal ions by semiconductor photocatalysis technology is based on the reduction of the metals by the generated electrons in the system:

$$M^{n+} + TiO_2(xe_{CB}^-) \rightarrow M^{(n-x)+} \quad (7)$$

It has been reported that Cu^{2+} can be reduced to Cu^0 by TiO_2 electrons [137,138]. Herrmann et al. [79] suggested that in the presence of TiO_2 suspensions Cu^{2+} ions are not reduced to Cu^0 but to Cu^{2+} even in the absence of molecular oxygen.

Recently, Mohamed et al. [22] studied the reduction of Cu^{2+}, Zn^{2+} and Mn^{2+} using stored electrons on TiO_2 nanoparticles. They found that Cu^{2+} ions were reduced through a two-electron transfer reaction to form Cu^0 nanoparticles which are detected by their typical surface Plasmon resonance band at 570 nm. They found also that neither the reduction of Zn^{2+} nor that of Mn^{2+} can be induced using stored TiO_2 electrons in these systems, attributing it to the thermodynamic infeasibility of the respective reduction processes.

Reduction of Ag^+. The photocatalytic reduction of metallic silver on semiconductors is amply documented for recovery, principally from waste photographic effluents, for the modification of semiconductors and also as the basis for photoimaging processes. Two limiting cases for the mechanism of colloidal metal particle formation have been proposed: [139] (a) aggregation of concurrently formed silver atoms:

$$mAg^0 \rightarrow Ag_m{}^0 \quad (8)$$

(b) a sequence of alternating electronic and ionic events which build up the Ag^0 particle in a similar way as the latent image cluster in silver halide photography:

$$Ag^0 + Ag^+ \rightarrow (Ag)_2{}^+ \xrightarrow{e^-} Ag_2 \xrightarrow{Ag^+} (Ag)_3{}^+ \xrightarrow{e^-} Ag_3 \rightarrow \cdots \rightarrow Ag_m \quad (9)$$

Recently, the primary events in the photocatalytic deposition of silver on nanoparticulate TiO_2 from ethanol solutions have been analyzed by picosecond-resolved laser flash photolysis [140].

Surface-trapped photoelectron states, probably Ti^{III}, and silver deposition could be observed on the same time scale. It was inferred that one-electron, inner sphere reduction of Ag^I by Ti^{III} is rate determining in the formation of the colloidal silver deposit, and that the particles grow by a sequence of alternating electronic and ionic events, as those proposed in Eq. (9). Other investigation focused on nanosecond laser flash photolysis studies of the reduction of silver ions by the TiO_2 conduction band electrons has also been reported

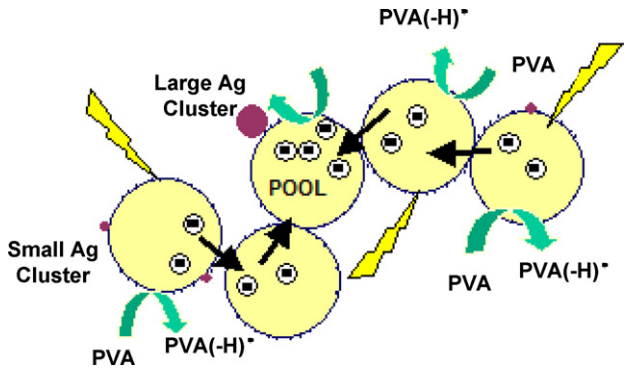

Fig. 15. Schematic of a proposed transfer of photogenerated electrons through a self-assembeled TiO_2 aggregates.
Reprinted with permission from Ref. [142].

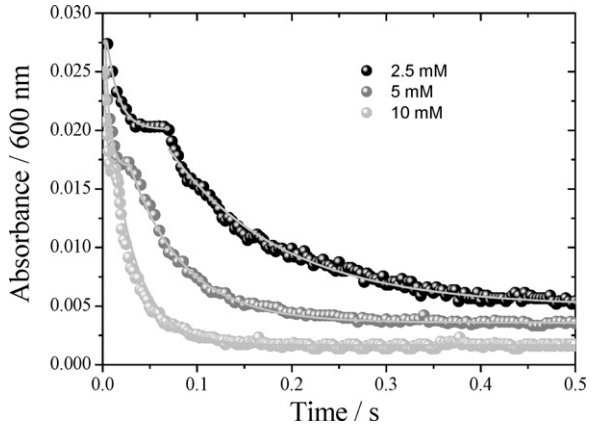

Fig. 16. Changes in the absorbance vs. time signals at 600 nm observed after 1:1 mixing of electrons loaded TiO_2 suspension ($[e_{TiO_2}^-] = 2.2 \times 10^{-4}$M, $2.4e_{TiO_2}^-$/particle) with Ar-saturated $AgClO_4$ aqueous solutions with different concentrations of Ag^+ ions, pH 2.7, solid lines present the first order fits.
Reprinted with permission from Ref. [23].

[141]. Friedmann et al. [142] have studied the primary processes during irradiating the system of TiO_2 nanoparticles and silver ions in presence of polyvinyl alcohol (PVA) using nanosecond XeF laser. They detected the photo deposition of metallic silver cluster containing ≥12 silver atoms on TiO_2 by detecting their absorption spectra with a maximum at 380 nm. Therefore it was suggested that the silver metal deposits formed an Ohmic contact with a highly doped TiO_2 semiconductors due to the creation of energy states as Ag+ ions were chemisorbed and Ag nuclei were formed on TiO_2. This study reports the first observation of antenna type effect for photocatalytic reduction reaction (c.f. Fig. 15) [142].

Mohamed et al. [23] have shown multi-phase kinetic decay curves for the TiO_2 electron absorbance due to the reduction of silver ions by electrons stored on TiO_2 nanoparticles (Fig. 16) [23]. This kinetic behavior was attributed to the multistep reduction of silver ions on the surface of TiO_2 followed by the transfer of excess electrons to the deposited silver particles. The above mechanism was found to be in good agreement with the work published by Wood et al. [143] and was detailed by the following equations:

$$n e_{TiO_2}^- + n Ag_{ads}^+ \rightarrow Ag_n^0 \quad \text{(reduction and nucleation)} \tag{10}$$

$$Ag_n^0 + Ag_{ads}^+ \rightarrow Ag_{n+1}^+ \quad \text{(autocatalytic growth)} \tag{11}$$

$$Ag_{n+1}^+ + e_{TiO_2}^- \rightarrow Ag_{n+1}^0 \tag{12}$$

$$Ag_{n+1}^0 + \overset{e_{TiO_2}^-, Ag^+}{\longrightarrow} Ag_x^0 \tag{13}$$

$$Ag_x^0 + Ag_y^0 \rightarrow Ag_{x+y}^0 \quad \text{(coalescence)} \tag{14}$$

$$Ag_{x+y}^0 + z e_{TiO_2}^- \rightarrow (Ag_{x+y}^0)^{z-}$$
$$\text{(transfer of electrons to Ag particles)} \tag{15}$$

$$(Ag_{x+y}^0)^{z-} + 2H_{ads}^+ \rightarrow (Ag_{x+y}^0)^{(z-2)-} + H_2 \quad (H_2 \text{ generation}) \tag{16}$$

5.3. Multiple electron transfer reactions

Upon incidence of high light intensities, the charge can accumulate at the semiconductor–electrolyte interface. Depending on the surface pre-treatment, the presence of surface states and the kinetics facilitate the interfacial electron transfer, the accumulated charge may sometimes be used to induce multiple electron transfer to or from an adsorbed substrate. This charge accumulation is critical in the redox reactions of simple inorganic molecule such as water oxidation, oxygen reduction, nitrogen reduction, nitrate reduction, chlorinated hydrocarbons reduction or CO_2 reduction. Multi-electron transfer reactions are important processes which avoid high-energy free radical intermediates and can yield desired reaction products under mild conditions. Multi-electron storage and hydrogen generation by light was achieved in aqueous dispersions of ultrafine TiO_2 particles when the amphiphilic viologen derivative N-tetradecyl-N′-methyl-4,4′-dipyridinium dichloride ($C_{14}MV^{2+}$) was used as an electron relay [80]. Two-electron reduction of $C_{14}MV^{2+}$ was coupled with H_2 generation in alkaline medium in the presence of Pt catalyst co-deposited onto the TiO_2 particle.

Obare et al. [107] studied multi-electron transfer reaction of organohalide pollutants at heme-functionalized nanocrystalline TiO_2 (Fig. 10). Using of this catalyst led to the formation of stable carbene products in greater than 60% yield.

Gao et al. [17] have studied the reactions of excess electrons in TiO_2 produced by radiolysis employing steady state and pulse radiolysis techniques. The authors analyzed the kinetics of the electron transfer reactions with several scavengers including NO_2^-, NO_3^-, O_2, H_2O_2 using different nanocrystal sizes. The authors found that the rates of electron reactions depend on particle size. Several scavengers including ClO_2^-, ClO_3^-, NO_2^-, and NO_3^- show decay of the TiO_2 electron predominantly by single pseudo-first order process. The rate of reaction of the above ions in the large nanocrystallites systems is 2–10 times faster than in the respective small particle systems. They found also that the rate of the reduction of the different scavengers tend to increase with the driving force.

Recently, Mohamed et al. [22] studied the multi-electron transfer reactions induced by stored electrons in TiO_2 nanoparticles employing stopped flow technique. They investigated the multi-electron reduction of common electron acceptors such as O_2, H_2O_2 and NO_3^-. The authors have observed that the rate of the electron absorbance decay depending on the concentration of the electron acceptors (c.f. Fig. 17) [22]. They found that the rate constant of the first initial decay ($k_I^{obs} = 2.0 \times 10^4\ M^{-1}\ s^{-1}$) and that of the second decay ($k_{II}^{obs} = 5.7 \times 10^3\ M^{-1}\ s^{-1}$) for the reaction of the stored TiO_2 electrons with molecular oxygen were similar to the values of the rate constants of the two slower processes k_{III} ($7.3 \pm 1.5 \times 10^3\ M^{-1}\ s^{-1}$) and k_{IV} ($1.0 \pm 0.2 \times 10^3\ M^{-1}\ s^{-1}$) as reported by Gao et al. [17] who studied the reaction of electrons formed by radiation chemical processes in small TiO_2 particles and who suggested that these slow processes are due to the reaction of excess TiO_2 electrons with molecular oxygen in the bulk.

Moreover, a multi-electron reduction of nitrate has recently received special attention in view of pollution control [144–148].

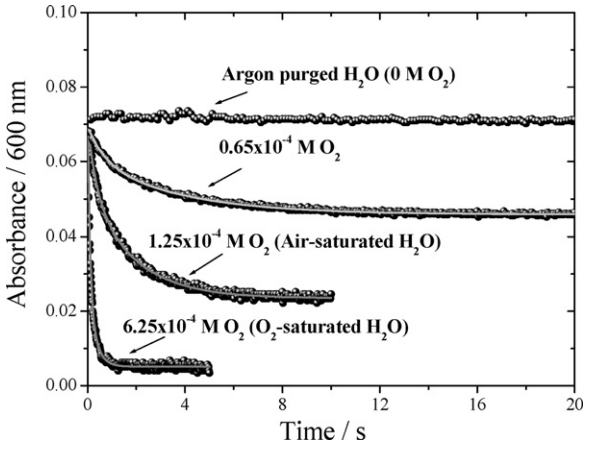

Fig. 17. (a) Time profiles of the decay of the $e_{TiO_2}^-$ absorbance at 600 nm ($[e_{TiO_2}^-] = 5.7 \times 10^{-4}$M, $6e_{TiO_2}^-$/particle) observed upon mixing of their aqueous suspension with different concentration of dissolved O_2 saturated aqueous solutions at pH 2.3 (HCl). The solid lines show the double exponential fits.

Reprinted with permission from Ref. [22].
© 2011 ACS

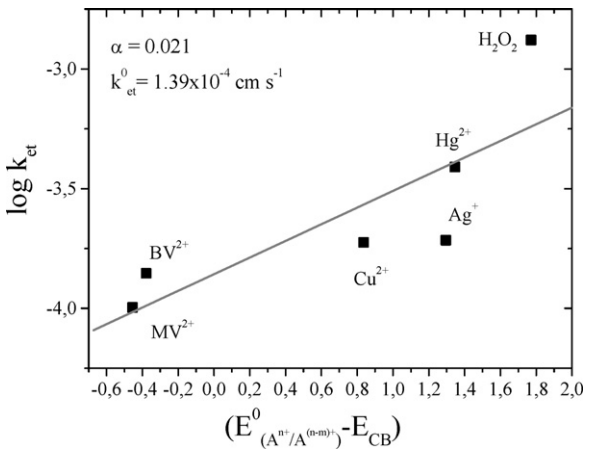

Fig. 18. Dependency of interfacial electron transfer rates on the driving forces. Adapted from Ref. [74].

Mohamed et al. [22] have found also that nitrate ions are reduced to ammonia through eight electron transfer and intermediate formation of molecular nitrogen according to the following equations [149]:

$$2NO_3^- + 12H^+ + 10e_{TiO_2}^- \rightarrow N_2 + 6H_2O \quad E_{redox} = 1.25V\,(vs.\ NHE) \tag{17}$$

$$N_2 + 4e_{TiO_2}^- + 5H^+ \rightarrow N_2H_5^+ \quad E_{redox} = -0.23V\,(vs.\ NHE) \tag{18}$$

$$N_2H_5^+ + 2e_{TiO_2}^- + 3H^+ \rightarrow 2NH_4^+ \quad E_{redox} = 1.27V\,(vs.\ NHE) \tag{19}$$

In contrast, Gao et al. [17] have observed one- instead of multi-electron reduction of nitrate ions by excess TiO_2 electrons using pulse radiolysis technique.

In recent publications [17–20], the reaction of electrons in TiO_2 with H^+ and water in the presence of noble metal coatings and employing pulse radiolysis technique have been investigated. Kasarevic-Popovic et al. [18] found that the reaction of TiO_2 electrons with H^+/H_2O is a pseudo first order reaction depending on Pt^0 and H^+ concentration. It was shown that the energy of the adsorbed hydrogen atoms on the Pt^0 surface is not sufficient to abstract hydrogen from 2-propanol. A similar observation was reported in Au/TiO_2 by Hussein and Rudham [19]. Behar and Rabani [20] studied the kinetics of hydrogen production upon the reaction of TiO_2 electrons with H^+ and water in presence of different surface metal catalyst (Pd^0, Pt^0 and Au^0). They found that when the TiO_2 nanoparticles are partially coated with Au^0 instead of Pd^0 or Pt^0, a higher than expected molecular hydrogen level is observed attributing this to a short chain reaction involving hydrogen abstraction from 2-propanol.

6. Relation between interfacial electron transfer rate constants and driving force

One of the most important parameters that affects the efficiency of the electron transfer reactions is the standard redox potential of the involved electron acceptor related to the standard redox potential of the conduction band electron because only those species with reduction potentials much more positive than the conduction band edge can be photoreduced.

The difference between the standard redox potential of the electron acceptor ($E_{(A^{n+}/A^{(n-m)+})}{}^0$) and the standard redox potential of the conduction band electrons corresponding to the Fermi energy (E_{CB}) is defined as the driving force of the electron transfer reaction.

The interfacial electron transfer rate constant k_{et} ($cm\,s^{-1}$) changes with the driving force ($E_{(A^{n+}/A^{(n-m)+})}{}^0 - E_{CB}$) according to Tafel equation (Eq. (11))

$$\log k_{et} = \log k_{et}{}^0 + \frac{\alpha}{0.059}\left(E_{\left(\frac{A^{n+}}{A^{(n-m)+}}\right)}{}^0 - E_{CB}\right) \tag{20}$$

where a is the transfer coefficient and $k_{et}{}^0$ the value of the rate constant for $E_{(A^{n+}/A^{(n-m)+})}{}^0 - E_{CB} = 0$. The interfacial electron transfer rate constant k_{et} is given by

$$k_2' = 4\pi R^2 k_{et}$$

(R is the sum of the radii of TiO_2 particle and the acceptor) (21)

where k_2' expressed in the unit $cm^3\,s^{-1}$, is related to the observed second order rate constant $k_2{}^{obs}$ ($M^{-1}\,s^{-1}$) by

$$k_2' = k_2{}^{obs} \times \frac{1000}{N_A} \quad (N_A = \text{the Avogadro's number}) \tag{22}$$

Table 1 summarizes the reactions, their redox potential, their observed second order rate constants ($k_2{}^{obs}$) obtained from the observed kinetic data [22–24,74] and their corresponding calculated electron transfer rate constants (k_{et}).

As no reaction between $e_{TiO_2}^-$ and Zn^{2+} or Mn^{2+} has been realized due to thermodynamic unfeasibility, the results of the reduction of other electron acceptors show the expected trend concerning the relationship between $\log k_{et}$ and the driving force of the electron transfer reaction taking the value of $E_{CB} = -0.5\,V_{NHE}$. This means that the electron transfer rate constants increases with increasing the driving force of the reduced couple as illustrated in Fig. 18 [74].

7. Future challenges and prospects

The main critical limitation to be achieved in photocatalysis is to increase of the efficiency of charge separation/transport in semiconductor nanoparticles. Although, several attempts have been made to improve the charge transfer efficiency including metal ions doping, surface modification and semiconductor coupling, the strategy to solve this problem need to be change. Firstly, the factors determining the electron transfer activity should be identified and a subsequent verification of how these factors influence their activity can be studied.

A major challenge still existing in semiconductor photocatalysis and need therefore to be examined is the correlation between the photocatalytic activities, the interfacial electron transfer and recombination kinetics. This correlation will help the understanding of the fundamental concepts of photocatalytic processes and hence result in understanding and industrialization of photocatalytic reactions as well as a rational design of the photocatalytic systems. To achieve this several insights and prospects should be addressed including:

(1) More detailed knowledge is needed about the electron transfer kinetics and mechanism under various parameters such as surface structure and area, crystal size and crystalline structure.
(2) Investigations of the electron transfer properties on well defined single crystals and correlate the data with those for polycrystalline nanoparticles.
(3) The ability to link between the theoretical and experimental kinetic study of the interfacial electron transfer in photocatalytic systems remains to be seen.
(4) Correlation of the temperature changes on the electron transfer kinetics for several photocatalytic systems still need to be studied in details.
(5) Many kinetics and mechanistic studies have been done on the thermodynamically favorable photo-induced electron transfer reactions such as photocatalytic reduction of transition metal ions or organic halides but little kinetic and mechanistic insights are known about the unfavorable reactions such as photocatalytic reduction of water or CO_2.

8. Summary

Electron transfer process plays a significant role in photocatalysis. The fundamental study of the dynamics of the charge transfer processes is important in the design of new photocatalysts as well as in the industrialization of the photocatalytic processes. This review highlights some significant insights obtained from the dynamics of interfacial electron transfer in photocatalysis. A focus was on the measurement of the interfacial electron transfer dynamics comprising different techniques including time resolved spectroscopy techniques, pulse radiolysis, stopped flow, EPR and photoluminscence. The factors affecting the effecincy of electron transfer have been discussed. The results reported suggest that the efficiency of electron transfer process and hence the overall photocatalytic process depends largely on the photocatalyst size, surface composition and morphology. The surface of the semiconductor particle can be modified by various methods such as deposition of noble metal clusters, doping of transition metal ions, surface complexation and semiconductor coupling.

Moreover, one of the most important parameters that affect the efficiency of the electron transfer reactions is the driving force of the electron transfer reaction. The electron transfer rate was found to increase with increasing the driving force. The new findings in the kinetics and of the mechanistic studies of some important electron transfer processes at TiO_2 nanoparticles such as reduction of viologen compounds, reduction of transition metal ions and multielectron reduction of organohalides, NO_3^-, H^+ and O_2 have been reviewed. The kinetic and mechanistic data have been compared using different techniques. TiO_2 nanoparticles act as electron pools for single- and multi-electron transfer processes. The electrons can be stored in the TiO_2 surface/bulk traps and then transfer to the acceptor molecules in one or multi-step processes. This review has illustrated how interfacial electron transfer perspectives can provide unique insights into the field of photocatalysis and motivate more knowledge sharing in research to cover major aspects of photocatalysis from fundamentals to applications.

Acknowledgements

Prof. Dr. Jean-Marie Hermann is gratefully acknowledged for his numerous contributions in the field of photocatalysis making this field attractive to many young scientists. Financial Support from Deutsche Forschungsgemeinschaft (DFG) is gratefully acknowledged (Grant no. BA 1137/8-1).

References

[1] D. Bahnemann, J. Cunningham, M.A. Fox, E. Pelizzetti, P. Pichat, N. Serpone, in: G.R. Helz, R.G. Zepp, D.G. Crosby (Eds.), Aquatic and Surface Photochemistry, Lewis Publishing, Boca Raton, London, Tokyo, 1994, pp. 261–316.
[2] D. Bahnemann, in: P. Boule (Ed.), The handbook of Environmental Chemistry, Environmental Photochemistry, vol. 2, Springer, Berlin, 1999, pp. 285–351.
[3] M.R. Hoffmann, S.T. Martin, W. Choi, D.W. Bahnemann, Chemical Reviews 95 (1995) 69–96.
[4] J.H. Carey, J. Lawrence, H.M. Tosine, Bulletin of Environment Contamination and Toxicology 16 (1976) 697–701.
[5] (a) R. Dillert, S. Vollmer, E. Gross, M. Schober, D. Bahnemann, Zeitschrift fur Physikalische Chemie 213 (1999) 141–147;
(b) R. Dillert, A.E. Cassano, R. Goslich, D. Bahnemann, Catalysis Today 54 (1999) 267–282.
[6] (a) J.-M. Herrmann, P. Pichat, Journal of the Chemical Society, Faraday Transactions 76 (1980) 1138–1146;
(b) J.-M. Herrmann, Helvetica Chimica Acta 84 (2001) 2731–2750.
[7] O.M. Alfano, D. Bahnemann, A.E. Cassan, R. Dillert, R. Goslich, Catalysis Today 58 (2000) 199–230.
[8] A. Henglein, Chemical Reviews 89 (1989) 1861–1873.
[9] M. Grätzel, Heterogeneous Photochemical Electron Transfer, CRC Press, Boca Raton, 1989.
[10] C.T. Kresge, M.E. Leonowicz, W.J. Roth, J.C. Vartuli, J.S. Beck, Nature 359 (1992) 710–712.
[11] S.A. Davis, S.L. Burkett, N.H. Mendelson, S. Mann, Nature 385 (1997) 420–423.
[12] W.-S. Chae, S.-W. Lee, Y.-R. Kim, Chemistry of Materials 17 (2005) 3072–3074.
[13] (a) H.B. Thu, M. Karkmaz, E. Puzenat, J.-M. Herrmann, Research on Chemical Intermediates 31 (2005) 449–461;
(b) P. Yang, D. Zhao, D.I. Margolese, B.F. Chmelka, G.D. Stucky, Nature 396 (1998) 152–155.
[14] D.W. Bahnemann, A. Henglein, J. Lili, L. Spanhel, Journal of Physical Chemistry 88 (1984) 709–711.
[15] D. Duonghong, J. Ramsden, M. Grätzel, Journal of the American Chemical Society 104 (1982) 2977–2985.
[16] M. Grätzel, A.J. Frank, Journal of Physical Chemistry 86 (1982) 2964–2967.
[17] R. Gao, A. Safrany, J. Rabani, Radiation Physics and Chemistry 67 (2003) 25–39.
[18] Z. Kasarevic-Popovic, D. Behar, J. Rabani, Journal of Physical Chemistry B 108 (2004) 20291–20295.
[19] F.H. Hussein, R. Rudham, Journal of the Chemical Society, Faraday Transactions 1 (1987) 2817–2825.
[20] D. Behar, J. Rabani, Journal of Physical Chemistry B 110 (2006) 8750–8755.
[21] H.H. Mohamed, R. Dillert, D.W. Bahnemann, Journal of Photochemistry and Photobiology A 217 (2011) 271–274.
[22] H.H. Mohamed, C.B. Mendive, R. Dillert, D.W. Bahnemann, Journal of Physical Chemistry A 115 (2011) 2139–2147.
[23] H.H. Mohamed, R. Dillert, D.W. Bahnemann, Journal of Physical Chemistry C 115 (2011) 12163–12172.
[24] H.H. Mohamed, R. Dillert, D.W. Bahnemann, Journal of Photochemistry and Photobiology A, in press.
[25] (a) Y. Tamaki, A. Furube, M. Murai, K. Hara, R. Katoh, M. Tachiya, Physical Chemistry Chemical Physics 9 (2007) 1453–1460;
(b) Y. Tamaki, A. Furube, M. Murai, K. Hara, R. Katoh, M. Tachiya, Journal of the American Chemical Society 28 (2006) 1416–1417.
[26] A.M. Peiro, C. Colombo, G. Doyle, J. Nelson, A. Mills, J.R. Durrant, Journal of Physical Chemistry B 110 (2006) 23255–23263.
[27] A.V. Emeline, V.K. Ryabchuk, N. Serpone, Journal of Physical Chemistry B 109 (2005) 18515–18521.
[28] Y. Wang, K. Hang, N.A. Anderson, T. Lian, Journal of Physical Chemistry B 107 (2003) 9434–9440.
[29] (a) A. Fujishima, X. Zhang, D.A. Tryk, Surface Science Reports 63 (2008) 515–582;
(b) T. Yoshihara, R. Katoh, A. Furube, Y. Tamaki, M. Murai, K. Hara, S. Murata, H. Arakawa, M. Tachiya, Journal of Physical Chemistry B 108 (2004) 3817–3823;
(c) A. Yamakata, T. Ishibashi, H. Onishi, Journal of Physical Chemistry B 105 (2001) 7258–7262;
(d) M. Murai, Y. Tamaki, A. Furube, K. Hara, R. Katoh, Catalysis Today 120 (2007) 214–219;
(e) K. Iwata, T. Takaya, H. Hamaguchi, A. Yamakata, T. Ishibashi, H. Onishi, H. Kuroda, Journal of Physical Chemistry B 108 (2004) 20233–20239.
[30] B.O. Regan, M. Grätzel, D. Fitzmaurice, Chemical Physics Letters 183 (1991) 89–93.
[31] G. Boschloo, D. Fitzmaurice, Journal of Physical Chemistry B 103 (1999) 2228–2231.

[32] A. Safrany, R. Gao, J. Rabani, Journal of Physical Chemistry 104 (2000) 5848–5853.
[33] C. Kormann, D.W. Bahnemann, M.R. Hoffmann, Journal of Physical Chemistry 92 (1988) 5196–5201.
[34] D.W. Bahnemann, C. Kormann, M.R. Hoffmann, Journal of Physical Chemistry 91 (1987) 3789–3798.
[35] D.P. Colombo, R.M. Bowman, Journal of Physical Chemistry 100 (1996) 18445–18449.
[36] R.B. Draper, M.A. Fox, Journal of Physical Chemistry 94 (1990) 4628–4634.
[37] N. Ikeda, K. Imagi, H. Masuhara, N. Nakashima, K. Yoshihara, Chemical Physics Letters 140 (1987) 481–486.
[38] N. Fukazawa, H. Fukumura, H. Masuhara, Chemical Physics Letters 222 (1994) 123–128.
[39] S. Hashimoto, N. Fukazawa, H. Fukumura, H. Masuhara, Chemical Physics Letters 223 (1994) 493–500.
[40] J. Moser, M. Grätzel, Journal of the American Chemical Society 105 (1983) 6547–6555.
[41] J.H. Fendler, F.C. Meldrum, Advanced Materials 7 (1995) 607–631.
[42] C.P. Collier, T. Vossmeyer, J.R. Heath, Annual Review of Physical Chemistry 42 (1998) 371–404.
[43] J.R. Heath, Science 258 (1992) 1131–1133.
[44] H. Weller, Angewandte Chemie International Edition in English 35 (1996) 1079–1081.
[45] R.P. Andres, J.D. Bielefeld, J.I. Henderson, D.B. Janes, V.R. Kolagunta, C.P. Kubiak, W.J. Mahoney, R.G. Osifchin, Science 273 (1996) 1690–1693.
[46] A.P. Alivisatos, EndeaVour 21 (1997) 56–60.
[47] K.V. Sarathy, P.J. Thomas, G.U. Kulkarni, C.N.R. Rao, Journal of Physical Chemistry B 103 (1999) 399–401.
[48] H. Weller, H.M. Schmidt, U. Koch, A. Fojtik, S. Baral, A. Henglein, W. Kunath, K. Weiss, E. Dieman, Chemical Physics Letters 124 (1986) 557–560.
[49] J.Z. Zhang, R.H. O'Neil, T.W. Roberti, Journal of Physical Chemistry 98 (1994) 3859–3864.
[50] V.L. Colvin, A.N. Goldstein, A.P. Alivisatos, Journal of the American Chemical Society 114 (1992) 5221–5230.
[51] T.W. Roberti, N.J. Cherepy, J.Z. Zhang, Journal of Chemical Physics 108 (1998) 2143–2151.
[52] N. Chestnoy, T.D. Harris, R. Hull, L.E. Brus, Journal of Physical Chemistry 90 (1986) 3393–3399.
[53] N. Herron, J.C. Calabrese, W.E. Farneth, Y. Wang, Science 259 (1993) 1426–1428.
[54] A. Sengupta, B. Jiang, K.C. Mandal, J.Z. Zhang, Journal of Physical Chemistry B 103 (1999) 3128–3137.
[55] J.E.B. Katari, V.L. Colvin, A.P. Alivisatos, Journal of Physical Chemistry 98 (1994) 4109–4117.
[56] J. Liu, X.D. Feng, G.E. Fryxell, L.Q. Wang, A.Y. Kim, M.L. Gong, Advanced Materials 10 (1998) 161–165.
[57] M.T. Reetz, W. Helbig, S.A. Quaiser, U. Stimming, N. Breuer, R. Vogel, Science 267 (1995) 367–369.
[58] R. Howe, M. Grätzel, Journal of Physical Chemistry 89 (1985) 4495–4499.
[59] G. Liu, et al., Environmental Science and Technology 33 (1999) 2081.
[60] T. Berger, M. Sterrer, O. Diwald, E. Knözinger, D. Panayotov, T.L. Thompson, J.T. Yates Jr., Journal of Physical Chemistry B 109 (2005) 6061–6068.
[61] D.C. Hurum, A.G. Agrios, K.A. Gray, Journal of Physical Chemistry B 107 (2003) 4545–4549.
[62] N.D. Abazović, M.I. Čomor, M.D. Dramićanin, D.J. Jovanović, S.P. Ahrenkiel, J.M. Nedeljković, Journal of Physical Chemistry B 110 (2006) 25366–25370.
[63] M. Anpo, M. Tomonari, M.A. Fox, Journal of Physical Chemistry 93 (1989) 7300–7309.
[64] K. Miyashita, S-i. Kuroda, S. Tajima, K. Takehira, S. Tobita, H. Kubota, Chemical Physics Letters 369 (2003) 225–231.
[65] N. Serpone, D. Lawless, R. Khairutdinov, Journal of Physical Chemistry 99 (1995) 16646–16654.
[66] H. Tang, H. Berger, P.E. Shmid, F. Levy, Solid State Communications 87 (1993) 847–850.
[67] M. Anpo, Research on Chemical Intermediates 9 (1989) 67–112.
[68] E.J. Johnson, J. Kafalas, R.W. Davies, W.A. Dyes, Applied Physics Letters 40 (1982) 993–995.
[69] V.Yu. Ivanov, Yu.G. Semenov, M. Surma, M. Godlewski, Physical Review B 54 (1996) 4696–4701.
[70] P.P. Paskov, P.O. Holtz, B. Monemar, J.M. Garcia, W.V. Schoenfeld, P.M. Petroff, Applied Physics Letters 77 (2000) 812–814.
[71] J. Zeman, G. Martinez, P.Y. Yu, K. Uchida, Physical Review B 55 (1997) R13428–R13431.
[72] W. Seidel, A. Titkov, J.P. André, P. Voisin, M. Voos, Physical Review Letters 73 (1994) 2356–2359.
[73] E. Poles, D.C. Selmarten, O.I. Mićić, A.J. Nozik, Applied Physics Letters 75 (1999) 971–973.
[74] H.H. Mohamed, PhD thesis, Instiut für Technische Chemie, Universität Hannover, 2011.
[75] W.Z. Wang, I. Germanenko, M.S. El-Shall, Chemistry of Materials 14 (2002) 3028–3033.
[76] A.L. Rogach, L. Katsikas, A. Kornowski, D. Su, A. Eychmüller, H. Weller, Berichte der Bunsen-Gesellschaft Physical Chemistry Chemical Physics 100 (1996) 1772–1778.
[77] C.B. Murray, C.R. Kagan, M.G. Bawendi, Annual Review of Materials Science 30 (2000) 545–610.
[78] R.L. Wells, W.L. Gladfelter, Journal of Cluster Science 8 (1997) 217–238.
[79] J.-M. Hermann, J. Disdier, P. Pichat, Journal of Physical Chemistry 90 (1986) 6028–6034.
[80] E. Vrachnon, M. Grätzel, A.J. McEvoy, Journal of Electroanalytical Chemistry 258 (1989) 193–205.
[81] K. Vinodgopal, P.V. Kamat, Environmental Science and Technology 29 (1995) 841–845.
[82] L. Brus, Journal of Physical Chemistry 90 (1986) 2555–2560.
[83] H. Gerischer, M. Luebke, Journal of Electroanalytical Chemistry 204 (1986) 225–232.
[84] L. Spanhel, H. Weller, Henglein, Journal of the American Chemical Society 109 (1987) 6632–6637.
[85] S. Hotchandani, P.V. Kamat, Journal of Physical Chemistry 96 (1992) 6834–6839.
[86] R. Vogel, P. Hoyer, H. Weller, Journal of Physical Chemistry 98 (1994) 3183–3188.
[87] C. Nasr, S. Hotchandani, W.Y. Kim, R.H. Schmehl, P.V. Kamat, Journal of Physical Chemistry B 101 (1997) 7480–7487.
[88] T. Hirakawa, P.V. Kamat, Journal of the American Chemical Society 127 (2005) 3928–3934.
[89] A. Zaban, O.I. Micic, B.A. Gregg, A.J. Nozik, Langmuir 14 (1998) 3153–3156.
[90] H. Tada, T.K. Teranishi, I. Yo-ichi, S. Ito, Langmuir 16 (2000) 3304–3309.
[91] V. Subramanian, E.E. Wolf, P.V. Kamat, Journal of the American Chemical Society 126 (2004) 4943–4950.
[92] M. Jacob, H. Levanon, P.V. Kamat, Nano Letters 3 (2003) 353–358.
[93] T. Hirakawa, P.V. Kamat, Langmuir 20 (2004) 5645–5647.
[94] V. Subramanian, E.E. Wolf, P.V. Kamat, Journal of Physical Chemistry B 107 (2003) 7479–7485.
[95] (a) P.V. Kamat, Journal of Physical Chemistry B 106 (2002) 7729–7747;
(b) P.V. Kamat, Pure and Applied Chemistry 74 (2002) 1693–1706.
[96] P.D. Cozzoli, E. Fanizza, R. Comparelli, M.L. Curri, D. Laub, A. Agostiano, Journal of Physical Chemistry B 108 (2004) 9623–9630.
[97] Y. Cong, J. Zhang, F. Chen, M. Anpo, Journal of Physical Chemistry C 111 (2007) 6976–6982.
[98] (a) Y. Park, W. Kim, H. Park, T. Tachikawa, T. Majima, W. Choi, Applied Catalysis B: Environmental 91 (2009) 355–361;
(b) J. Fang, F. Wang, K. Qian, H. Bao, Z. Jiang, W. Huang, Journal of Physical Chemistry C 112 (2008) 18150–18156.
[99] Y. Huang, W. Ho, S. Lee, L. Li, G. Zhang, J.C. Yu, Langmuir 24 (2008) 3510–3516.
[100] J.H. Pan, X. Zhang, A.J. Du, D.D. Sun, J.O. Leckie, Journal of the American Chemical Society 130 (2008) 11256–11257.
[101] G. Liu, Z. Chen, C. Dong, Y. Zhao, F. Li, G.Q. Lu, H.-M. Cheng, Journal of Physical Chemistry B 110 (2006) 20823–20828.
[102] (a) R.M. Navarro, F.d. Valle, J.A.V. de la Mano, M.C.A. Galvan, Advances in Chemical Engineering 36 (2009) 111–143;
(b) A.L. Linsebigler, G. Lu, J.T. Yates, Chemical Reviews 95 (1995) 735–758;
(c) S. Hotchandani, P.V. Kamat, Journal of Physical Chemistry 96 (1992) 6834–6843.
[103] C. Nasr, S. Hotchandani, P.V. Kamat, Journal of Physical Chemistry B 102 (1998) 10047–10056.
[104] C. Nasr, P.V. Kamat, S. Hotchandani, Journal of Electroanalytical Chemistry 420 (1997) 201–207.
[105] C. Nasr, S. Hotchandani, W.Y. Kim, S.R.H. Chmehl, P.V. Kamat, Journal of Physical Chemistry B 101 (1997) 7480–7487.
[106] O.V. Makarova, T. Rajh, M.C. Thurnauer, A. Martin, P.A. Kemme, D. Cropek, Environmental Science and Technology 34 (2000) 4797–4803.
[107] (a) S.O. Obare, T. Ito, G.J. Meyer, Journal of the American Chemical Society 128 (2006) 712–713;
(b) S.O. Obare, T. Ito, M.H. Balfour, G.J. Meyer, Nano Letters 3 (2003) 1151–1153.
[108] T. Ito, G.J. Meyer, Environmental Engineering Science 24 (2007) 31–44.
[109] T. Ito, PhD Thesis, Johns Hopkins University, 2006.
[110] (a) A.A. Ismail, D.W. Bahnemann, I. Bannat, M. Wark, Journal of Physical Chemistry C 113 (2009) 7429–7435;
(b) A.A. Ismail, D.W. Bahnemann, Journal of Materials Chemistry 21 (2011) 11686–11707.
[111] D.M. Antonelli, J.Y. Ying, Angewandte Chemie International Edition in English 34 (1995) 2014–2017.
[112] X. Wang, R.A. Caruso, Journal of Materials Chemistry 21 (2011) 20–28.
[113] M. Andersson, H. Birkedal, N.R. Franklin, T. Ostomel, S. Boettcher, A.C. Palmqvist, G.D. Stucky, Chemistry of Materials 17 (2005) 1409–1415.
[114] X. Wang, J.C. Yu, H.Y. Yip, L. Wu, P.K. Wong, S.Y. Lai, Chemistry – A European Journal 11 (2005) 2997–3004.
[115] A.K. Sinha, K. Suzuki, Journal of Physical Chemistry B 109 (2005) 1708–1714.
[116] J.H. Schattka, D. Shchukin, G. Jia, J.M. Antonietti, R.A. Caruso, Chemistry of Materials 14 (2002) 5103–5108.
[117] R.J. Tayade, R.G. Kulkarni, R.V. Jasra, Industrial and Engineering Chemistry Research 45 (2006) 5231–5238.
[118] D. Jing, Y. Zhang, L. Guo, Chemical Physics Letters 415 (2005) 74–78.
[119] H. Choi, M.G. Aantoniou, M. Pelaez, A.A. Delacruz, O.A. Shoemaker, D.D. Dionysiou, Environmental Science and Technology 41 (2007) 7530–7535.
[120] E. Ghadiri, N. Taghavinia, S.M. Zakeeruddin, M. Grätzel, J.-E. Moser, Nano Letters 10 (2010) 1632–1638.
[121] M. Grätzel, J. Moser, Proceedings of the National Academy of Sciences 80 (1983) 3129–3132.
[122] A.I. Krasna, Photochemistry and Photobiology 31 (1980) 75–82.

[123] J.R. Darwent, Journal of the Chemical Society, Chemical Communications 17 (1980) 805–807.
[124] R.J. Crutchley, A.B.P. Lever, Journal of the American Chemical Society 102 (1980) 7128–7129.
[125] T. Tanno, D. Wöhrle, M. Kaneko, A. Yamada, Berichte der Bunsen-Gesellschaft Physical Chemistry Chemical Physics 84 (1980) 1032–1034.
[126] D. Meisel, W.A. Mulac, M.S. Matheson, Journal of Physical Chemistry 85 (1981) 179–187.
[127] I. Okura, N. Kim-Thuan, Journal of the Chemical Society, Faraday Transactions 1 (77) (1981) 1411–1415.
[128] A. Harriman, G. Porter, M.C. Richoux, Journal of the Chemical Society, Faraday Transactions 2 (77) (1981) 833–844.
[129] J.S. Bus, S.D. Aust, J.E. Gibson, Biochemical and Biophysical Research Communications 58 (1974) 749–752.
[130] A.G. Evans, N.K. Dodson, N.H. Rees, Journal of the Chemical Society Perkin Transactions II 2 (1976) 859–863.
[131] T.W. Ebbesen, G. Ferraudi, Journal of Physical Chemistry 87 (1983) 3717–3721.
[132] G.A. Somorjai, Y.G. Borodko, Catalysis Letters 76 (2001) 1–5.
[133] Z. Ma, F. Zaera, in: B.R. King (Ed.), Encyclopedia of Inorganic Chemsitry, second ed., John Wiley & Sons Ltd., West Sussex, 2005, pp. 1768–1784.
[134] M. Che, C.O. Bennett, Advances in Catalysis 36 (1989) 55–172.
[135] G.C. Bond, Accounts of Chemical Research 26 (1993) 490–495.
[136] G.A. Somorjai, Catalysis Letters 7 (1990) 169–182.
[137] J.-F. Lambert, M. Che, Journal of Molecular Catalysis A 162 (2000) 5–18.
[138] H. Reiche, W.W. Dunn, A.J. Bard, Journal of Physical Chemistry 83 (1979) 2248–2251.
[139] M.D. Ward, A.J. Bard, Journal of Physical Chemistry 86 (1982) 3599–3805.
[140] M.I. Litter, Applied Catalysis B: Environmental 23 (1999) 89–114.
[141] M.R.V. Sahyun, N. Serpone, Langmuir 13 (1997) 5082–5088.
[142] D. Friedmann, H. Hansing, D.W. Bahnemann, Zeitschrift fur Physikalische Chemie 221 (2007) 329–348.
[143] A. Wood, M. Giersig, P. Mulvaney, Journal of Physical Chemistry B 105 (2001) 8810–8881.
[144] K.T. Ranjit, B.J. Viswanathan, Journal of Photochemistry and Photobiology A 108 (1997) 73–78.
[145] K.T. Ranjit, B.J. Viswanathan, T.K. Varadarajan, Journal of Materials Science Letters 15 (1996) 874–877.
[146] K.T. Ranjit, T.K. Varadarajan, B.J. Viswanathan, Journal of Physical Chemistry A 89 (1995) 67–68.
[147] F. Zhang, Y. Pi, J. Cui, Y. Yang, X. Zhang, N. Guan, Journal of Physical Chemistry C 111 (2007) 3756–3761.
[148] M. Halmann, K. Zuckerman, Journal of the Chemical Society, Chemical Communications (1986) 455–462.
[149] B. Douglas, D.H. McDanial, J.J. Alexander, Concepts and Model of Inorganic Chemistry, second ed., Wiley, New Yourk, 1983.